When Being Soft Makes You Tough: A Collision Resilient Quadcopter Inspired by Arthropod Exoskeletons

Ricardo de Azambuja[1,2] Hassan Fouad[2], and Giovanni Beltrame[2]

arXiv:2103.04423v1 [cs.RO] 7 Mar 2021

***Abstract*—Flying robots are usually rather delicate, and require protective enclosures when facing the risk of collision. High complexity and reduced payload are recurrent problems with collision-tolerant flying robots. Inspired by arthropods' exoskeletons, we design a simple, easily manufactured, semi-rigid structure with flexible joints that can withstand high-velocity impacts. With an exoskeleton, the protective shell becomes part of the main robot structure, thereby minimizing its loss in payload capacity. Our design is simple to build and customize using cheap components and consumer-grade 3D printers. Our results show we can build a sub-$250\,\mathrm{g}$, autonomous quadcopter with visual navigation that can survive multiple collisions at speeds up to $7\,\mathrm{m\,s^{-1}}$ that is also suitable for automated battery swapping, and with enough computing power to run deep neural network models. This structure makes for an ideal platform for high-risk activities (such as flying in a cluttered environment or reinforcement learning training) without damage to the hardware or the environment.**

I. Introduction

The world is an unforgiving place and any robot will sooner or later face a collision. Complex sensors and computational methods are usually employed to avoid collisions, while nature takes a different approach, and in many cases animals embrace collisions instead of avoiding them. One example of such amazing behaviour comes from a well known arthropod: the cockroach. It is capable of achieving faster direction transitions by hitting its head against walls instead of slowing down and turning [1].

Uncrewed Aerial Vehicles (UAVs) can also take advantage of collisions and physically interact with the environment. This idea was shown to reduce the control complexity when flying at low altitude surrounded by trees [2], to allow a drone to fly only using its sense of touch [3], and to enable a swarm of pico quadcopters to go through confined spaces by crashing onto each other and the environment. Similarly, collisions can be used to enable sharper changes in the flight direction of small UAVs [4]. Recent studies have presented contact–based navigation [3], [5] and even a complete collision inertial odometry algorithm that uses collisions to constrain velocity drift [6]. Collision tolerance is also extremely useful for application of reinforcement learning on real robots without excessive safety restrictions [7]

In general, the main strategy to endow UAV designs with collision resilience has been the use of protective structures like cages and bumpers, mostly made of rigid materials [6], [8], [9], [2], [10], [11], [12]. Rigid protective structures for UAVs also evolved into designs that allowed some level of movement like a sphere containing a gimbal or a cylinder that is capable of rolling around its main axis [2], [10], [11], [12], but their drawbacks are increased weight, mechanical complexity, and lack of energy absorption for force components perpendicular or aligned to the axis of rotation.

Protective structures do not need to be rigid: the commercial UAV Parrot AR.Drone 2.0 has a soft external hull made of Expanded Polypropylene (EPP) for protecting propellers and main body against collisions. A problem that comes from the use of EPP is its low specific stiffness (i.e. the stiffness to weight ratio) making it too heavy for high-energy impacts [13]. However, Parrot's soft protective hull seems quite successful for indoor and low-energy impacts, tolerating at least up to 11,500 of such low-energy collisions [7]. In addition to EPP, soft protective structures for UAVs have been designed using different materials. An origami rotatory protection, made by precision laser-cutting and folding very thin plastic sheets, was shown to withstand impacts up to 2m/s [14].

Carbon fiber structures are very popular with drone frame designers because of their steel-like stiffness. However, it is also possible to take advantage of their elastic behaviour (Euler-springs) to design flexible protective cages [13], [15]. Nevertheless, the high strength of carbon fiber limits its stand-alone energy absorption applications to long and thin struts, increasing weight. Additionally, the energy stored inside of carbon fiber rods could be dangerously released in case of material failure [16].

Weight reduction can be seen as a simple and effective collision resilience strategy [4]. Small weight and size comes with disadvantages such as smaller motors, leading to smaller payloads and limited ability to counter disturbances. Payload limitations also restrict battery size, computational power and ultimately the possible useful applications of the platform.

A frame that is capable of absorbing energy during a collision while protecting sensitive parts, by changing its shape or employing non-destructive deformation, is another option for collision resilient drones. However, previous strategies based on flexible frames [17], [16], [18], [19] make it very difficult for the UAV to instantly recover from a hard collision because they all lead to an inevitable fall to the ground as they automatically fold or disconnect the motors.

Yet, one significant advantage of not using any special structure to keep propellers from touching obstacles [16],

[1] University of Edinburgh.
[2] Polytechnique Montréal.
Contact: me@ricardodeazambuja.com

[18], [19] is the increase in payload capability. However, unprotected propellers don't allow UAVs to physically interact with the external world, even considering the use of special flexible propellers [20], as the decrease in thrust and torque from a bent propeller during a collision could still destabilize the UAV.

Depending on the design options adopted for helping withstand collisions, the weight of an UAV can vary from a few grams to kilograms. While a pico drone can weigh only 25g [4], the total mass of a much more complex drone based on gimbals can reach around 2kg when the batteries are included [10], [11]. Still, most regulatory agencies around the world take the $250\,\mathrm{g}$ value as the limit for an UAV that is considered safe without the need of special licenses or authorisations before flying.

From all research projects mentioned, only a few managed to keep the total weight below this threshold [4], [14], [16], [18], and they all employ high-speed coreless brushed DC motors limiting their payload, total flight time and lifespan [21]. Moreover, those sub-$250\,\mathrm{g}$ UAVs have a very limited maximum payload, on-board computing and sensing capacity, requiring external control and/or an external motion capture systems. In fact, even disregarding the collision resilience aspects, it is still quite rare to find research drones under $250\,\mathrm{g}$ that offer the extra power to run computationally complex software on-board (e.g. object detection using neural network models [22], [23]) and to be programmed without the need to make direct changes to the main flight controller firmware.

Looking at solutions to these issues provided by nature, arthropods can be a rich source of inspiration for innovative UAV designs. The most distinguished characteristics of arthropods is the presence of jointed appendages, body segmentation and a nonliving external skeleton, called an *exoskeleton*. An exoskeleton has a dual-purpose: *it works as support and protective structure*. The exoskeleton is responsible to support and give shape to the arthropods' body and it is an important protection against external attacks or injuries. Nevertheless, it is not necessarily fully rigid, mixing rigid segments connected by flexible joints, allowing bending and compression [24].

Structures inspired by exoskeletons are an interesting proposition for impact resilient frames: they mix rigidity with flexibility to absorb collision energy and protect sensitive components. For an UAV, such a mixed structure helps increasing the maximum payload and could afford a simpler control system that allows the UAV to physically interact with the environment without damage.

Despite the extensive effort from the research community to improve the collision resilience in UAVs, the use of an easy to manufacture, exoskeleton-like structure mixing rigid and soft materials in a sub-$250\,\mathrm{g}$ UAV has not been studied or presented yet. Two innovative works explored truly flexible frames [16], [18], but they only offered protection against collisions in one direction while leaving propellers mostly exposed, and they were not easy to manufacture without specialized materials or tools. Moreover, all collision-resilient systems under $250\,\mathrm{g}$ had bare minimum payload capacity, restricting their on-board computational power and their ability to fly autonomously without an external computer. Finally, their batteries had to be manually connected and extracted, making it very difficult to design an automated battery swapping station.

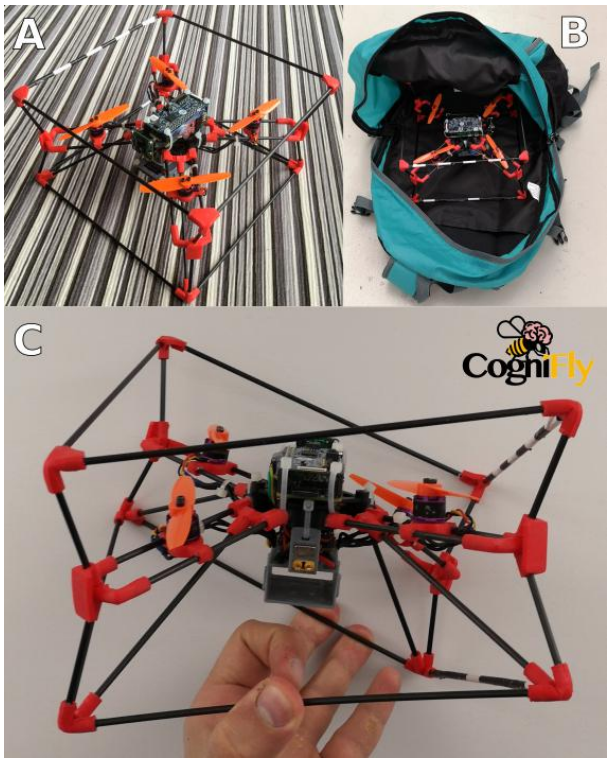

Fig. 1: CogniFly (A, B and C) is an under-$250\,\mathrm{g}$, open source, collision resilient UAV that measures only 210 x 210 x 120mm (B), and is capable of autonomous flight (no GPS) while running custom deep neural networks models like object detectors only using its on-board equipment. It is inspired by arthropods exoskeleton blending 3D printed soft parts (TPU 95A, in red) with ordinary ABS/PLA pieces (black/gray) and commercial, off-the-shelf pultruded carbon fiber rods (3mm diameter). It bends under certain loads while keeping sensitive parts intact (C).

In this work we present the CogniFly, shown in Figure 1, an under-$250\,\mathrm{g}$, open source, small size and collision resilient quadcopter. Inspired by chitinous exoskeletons, the CogniFly employs an exoskeleton made of carbon fiber rods, connected with 3D printed soft joints. This exoskeleton is designed in such a way that it provides sufficient protection for sensitive components, while providing effective passive damping of impacts, rendering the CogniFly a collision-resilient drone. Additionally, the CogniFly has several attractive traits like its repairability and versatility. CogniFly's repairability stems from its design that depends on readily available carbon fiber rods and 3D printers. Moreover, its versatility is manifested in its ability to run fairly complex algorithms and custom deep neural networks models despite of its relatively small size, which opens the door for several potential applications like agriculture, subterranean exploration, drone swarming and many others.

II. Materials and methods

In this section we briefly describe the experimental setup adopted in this work, as well as the procedure of obtaining the adequate parameter values for the proposed mass spring damper model.

A. Onboard payload composition

CogniFly uses a Raspberry Pi Zero W as its high level controller, to take advantage of low power consumption and the large community that already exists around RaspberryPi single-board computers. AI on the edge is supported by the neural compute engine Intel Movidius in the shape of Google's AIY Vision Bonnet[1], allowing it to capture images and directly run complex deep neural models like object detectors while still offering a good compromise in terms of weight and power consumption. Table I presents a comparison between the configuration used in CogniFly with other configurations for specialized hardware for AI on edge.

The CogniFly also features a flight controller (Kakute F7 Mini running iNav), Optical Flow (PMW3901) and Time-of-Flight (VL53L0X) sensors, thus CogniFly can operate autonomously in a GPS-denied environment from its own on-board hardware using a bespoke open source library called YAMSPy[2].

The payload, along with the motors, are powered by a 3S 650 mAh Lipo battery allowing a maximum flight time of around 5min. The battery holder and sleeve are designed in such a way to enable easy and quick extraction and insertion of batteries, depicted in Figure 2, which we plan as being a stepping stone towards designing small-sized portable battery swap stations for extended energy autonomy of CogniFly. Owing to the relatively small size of the CogniFly, such battery swap station will be able to fit on different commercially available ground robots (e.g. RoverPro from RoverRobotics or Jackal from Clearpath).

B. Free fall experiments

We perform a series free fall tests and record the absolute acceleration (Eq. 1) from the onboard accelerometer (Figure 3). We carry out these tests for assessing the CogniFly's ability to protect the payload from high energy impacts after a free fall, as well as highlighting the ability of the CogniFly's flexible structure to absorb impact by comparing the acceleration recorded from a full CogniFly and only the rigid central part of the frame, which holds the flight controller and the battery, made of ABS.

$$|acc| = \sqrt{{acc_x}^2 + {acc_y}^2 + {acc_z}^2} \tag{1}$$

For these tests, the main payload is replaced with a simpler one for recording absolute acceleration data. This test module is comprised of an accelerometer module (ADXL377) and a data logger module (Feather M0 Express) and it is presented in Figures 4 and 3. Weight of both configurations (flexigle and rigid) was set to be almost the same, resulting in the flexible CogniFly with $241\,\mathrm{g}$ and the ABS structure with $239\,\mathrm{g}$.

[1]https://aiyprojects.withgoogle.com/vision
[2]https://github.com/thecognifly/YAMSPy

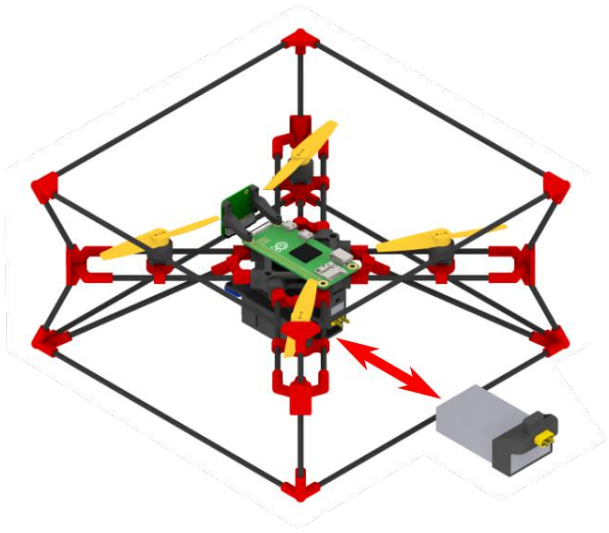

Fig. 2: CogniFly was designed from ground up for automatic battery swapping. Its battery (light gray, on the right) uses a 3D printed lid attached to the XT30 connector allowing the battery to easily slide in and out. Two magnets (NdFeB) are added to increase holding force, so the battery doesn't disconnect during impacts.

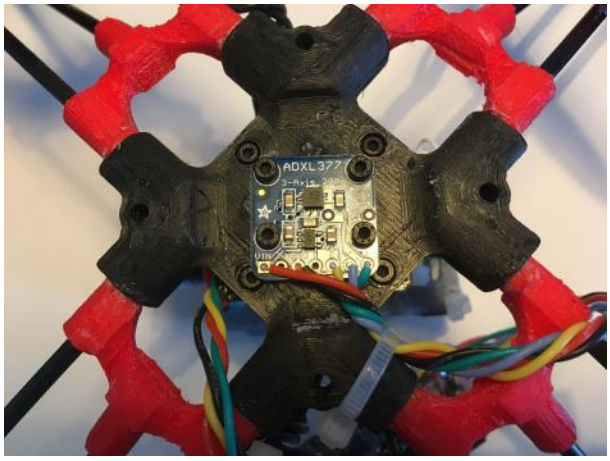

Fig. 3: Accelerometer (Adafruit ADXL377, 3-Axis, ±200G, 500Hz) was rigidly attached to the center of the drone. A Feather M0 Express running a custom firmware sampled (1kHz) and stored the data. For these experiments, we added a battery for the datalogger totalling 241g.

C. Mass-spring-damper model

We model the impact absorbing aspect of the CogniFly as a mass-spring-damper system that is described by

$$m\ddot{x} + c\dot{x} + kx = F \tag{2}$$

where $m > 0$ is the mass of the drone, $c > 0$ is the equivalent damping coefficient of the damper and $k > 0$ is the equivalent stiffness of the spring. A schematic of the system is depicted in Figure 14. Moreover, we augment the previous model with a first order butterworth low pass filter with a cutoff frequency of 500Hz to model the sampling latency of

TABLE I: Comparison of lightweight specialized hardware for AI on the edge.

	RPI Zero W + Google AIY Vision Bonnet	**NVidia Xavier NX**	**JeVois**	**Bitcraze AI-DECK**
CPU	1-core ARM1176 @ 1GHz + 1-core SAM D09@ 48MHz	6-core ARMv8.2 @ 1400MHz/1900MHz	4-core Allwinner A33 @ 1.34GHz	ESP32 @2.4GHz
GPU	VideoCore 4 @ 250MHz + 12-core Myriad 2 VPU 2450 @ 933 MHz	384-core Volta @ 1100MHz	Dual-core MALI-400 GPU	8+1-core @ 250MHz
RAM	512MB + 4 GB	8GB	256MB	64Mb
Flash	SDCARD	16GB (depends on carrier board)	SDCARD	512Mb
Power	1.2W (measured while running YAMSPy and an object detector)	10/15W	<4W	Up to 1.5W (5V, 300mA)
Weight	26g (includes one Raspicam V2)	24g (no heatsink, carrier board or camera)	17g (includes camera)	4.4g (includes camera)

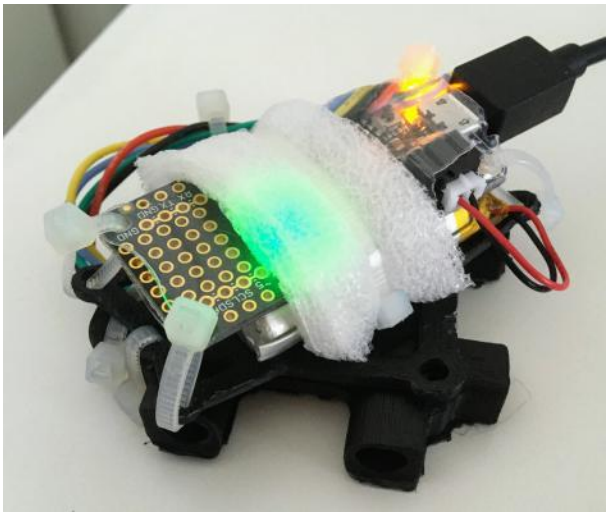

Fig. 4: For the crash landing experiments, thanks to CogniFly's modularity, we could build a specialized module (above) with an accelerometer (ADXL377) and a data logger (Feather M0 Express) that would directly fit into the rigid part of its frame, depicted in Figure 8. For debugging, only the module had to lay on a desk to connect it to a computer.

the accelerometer breakout board used. The overall structure is depicted in Figure 14.

In order to obtain the parameters in equation 2, we first put equation 2 in the following form

$$\begin{bmatrix} \dot{x} \\ \dot{v} \end{bmatrix} = \begin{bmatrix} 0 & 1 \\ -\frac{k}{m} & -\frac{c}{m} \end{bmatrix} \begin{bmatrix} x \\ v \end{bmatrix} + \begin{bmatrix} 0 \\ \frac{1}{m} \end{bmatrix} F \tag{3}$$

and then use Scipy (v.1.16) signal processing tool *lsim* to solve the system (3) to obtain the velocity and displacement of the payload's centre of gravity as a function of the initial displacement, velocity, and the parameters k, c to be estimated. In order to model the conditions at moment of impact, we set the external force F to gravity, the initial displacement to zero and the initial velocity to the value of velocity just before impact (which can be conservatively estimated by solving for the velocity of a free falling body without air drag). From the results obtained, we finally calculate the acceleration by a simple integration.

The value of the equivalent stiffness k is obtained through a static deformation test by deforming the payload to a known displacement, while measuring the required force for such deformation. Using the collected data, we fit a linear model, constraining the intersection to weight of the structure, so that the slope will be the value of k. Figure 5 shows the relation between the applied force and the resulting displacement, as well as the linear fit relation.

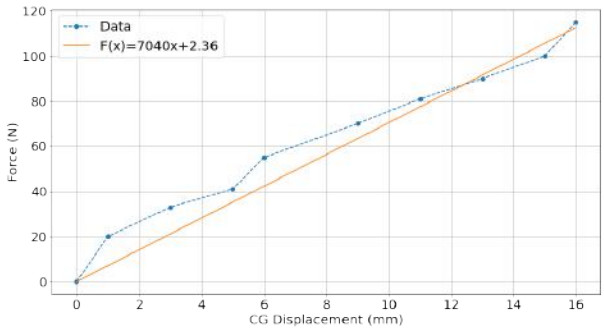

Fig. 5: Static stiffness measurement and spring model calculated. Data was collected using a dynamometer while the equilibrium ($x = 0$) was $W = mg = 2.36N$.

The loss function (z) created to estimate the equivalent damping c uses the Mean Square Error (MSE) between the mass-spring-damper model (after passing through a 1st order Butterworth low-pass filter, Figure 14) and the collected acceleration data from the end of the free fall until the peak of the measured absolute acceleration (Eq. 1) for all experiments (50, 100 and 150 cm). However, as the number of trials for each experiment is different (101, 97 and 89, respectively), the final value is weighted accordingly to avoid a bias towards the number of trials. For the visualization of the loss function, the natural logaritm (*cauchy* loss, $L(z) = ln(1+z)$) was used and the Figure 6 shows its visualization.

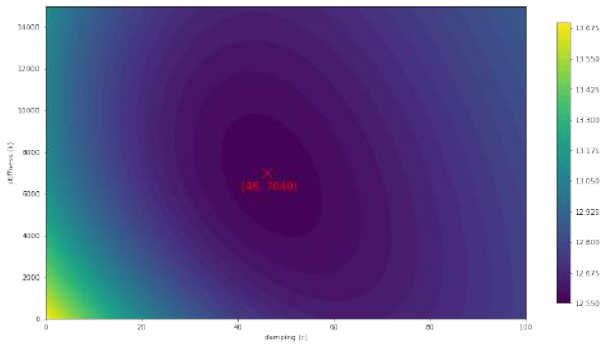

Fig. 6: The contour plot of the loss function ($ln(1 + z)$) used in the minimization problem for the selection of the damping coefficient c. The cross (red) marks the selected coefficient values ($c = 46$ and $k = 7040$) for a loss of 12.559883.

The minimization of the loss function was carried out using Scipy (v1.5.3) Optimize *minimize*, with *Nelder-Mead* method, default arguments and initial values of $c = 50$ and $k = 7040$. It resulted in a loss value of $L = 12.559869$ and coefficients $c = 46.31500979$ and $k = 6996.12384851$. However, as the loss value was very close to the one using

the static k experimentally measured ($L = 12.559883$), we adopted the coefficients $c = 46$ and $k = 7040$ for our model. The experimental data, together with the respective Jupyter notebooks, will be available at the project's github repository.

We use the proposed mass-spring-damper model to calculate the percentages of the energy that goes into different parts of the system during the impact, which is depicted in Figure 17. To construct such plot, we consider the kinetic energy ($E_k = \frac{1}{2}mv^2$) of the drone at the beginning of the impact (end of the free fall) as being the total energy of the system. Therefore, we have two possible situations: the payload never touches the ground ($x < 16mm$) or the payload hits the ground ($x \geq 16mm$).

In the situations where the payload (the bottom part of the battery holder in our experiments) never touches the ground (drop altitudes up to 100cm), the final kinetic energy at the point of maximum displacement is zero (the movement is about to reverse) and the total energy is split between stored in the spring ($E_s = \frac{1}{2}kx^2$) and dissipated by the damper ($E_d = E_k - E_s$).

Our mass-spring-model can't take into account the collision between the payload and the ground (drop altitudes from $150\,\mathrm{cm}$ and above) and it is only valid until $x \leq 16mm$. Therefore, in these situations we calculate the energy dissipated by the damper considering the difference between the initial kinetic energy (E_k) and the kinetic energy when $x = 16mm$. This way we know, in the worst scenario, the energy that will be dissipated during the *rigid* collision (payload hits the ground) will be the same as the kinetic energy available at $x = 16mm$ (represented by the red bars in Figure17) to indicate the severity of the payload impact to the ground.

III. Results

Our prototype of the CogniFly is light weight, easy to manufacture, it has powerful on-board computing, and can absorb and dissipate multiple high-energy impacts. In this section, we give a description of its overall structure, components, and design choices. Moreover, we assess the prototype's ability to absorb impacts through a series of free fall tests from different altitudes, looking at center of gravity displacements and to comparing with a similar device with a more rigid ABS plastic structure.

Finally, we model the behaviour of the prototype during impacts as a mass-spring-damper system (see materials and methods), and we show the results of the parameter estimation and the ability of such relatively simple model to predict absolute accelerations of the drone during impact.

A. CogniFly Composition

One of the main features of CogniFly is that it weighs less than $250\,\mathrm{g}$, while still having enough room for a payload capable of running deep neural network models. In this section, we describe the main structural features of the CogniFly, as well as its main onboard components that give it versatility and flexibility in different types of missions.

1) Structural design: The CogniFly takes inspiration from arthropods' exoskeletons in that its protective cage is a part of the overall structure. The primary design choice we adopt is to reduce the structural components for building the exoskeleton as much as possible to reduce weight. In our design, we opt for a box-like exoskeleton shape made of carbon fiber rods as depicted in Figure 1.

The protective role of the exoskeleton calls for the ability to damp and distribute impact energy, which leads to our second design choice, namely, using 3D printed flexible joints to connect the carbon fiber rods. These joints are made of TPU 95A and its flexibility and ductility provide sufficient damping for impacts, helping CogniFly survive impacts at speeds up to 7m/s. This material enables the drone to be generally flexible, as shown in Figure 1-C, which helps dissipating impact energy, while keeping the shape of its central part, allowing operation with a regular flight controller. It is worth mentioning that the dimensions of the outer exoskeleton are chosen to reduce the probability of contact between the internal components (payload, motors, etc.) and the exoskeleton.

To verify that the CogniFly frame truly behaves as an exoskeleton, we simulated the deformation of the frame under loads with and without the cage-like external protective parts of its structure. The results show smaller deformations when the external parts of CogniFly's frame are installed (Figure 7), reinforcing the idea the protection also support structural loads, and does not come at the expense of reduced payload.

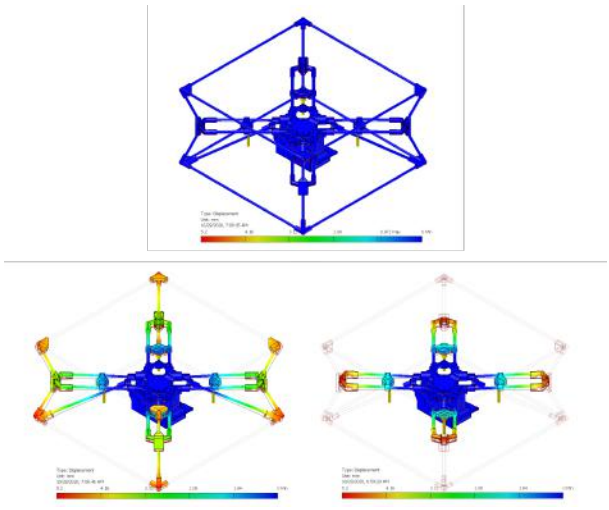

Fig. 7: To illustrate how CogniFly's frame behaves as an exoskeleton, four individual loads (100N) are applied where motors are assembled to analyse the displacement with and without the external protective structure (i.e., the equivalent of a cage). As a simplification because of the limitations of linear static analysis, TPU 3D printed parts parameters are replaced with standard ABS, and carbon fiber with standard titanium. Without the cage, the maximum deformations increase more than five times (from less than 1mm to more than 5mm).

2) Manufacturability: One important aspect in the CogniFly's design is the ease of manufacturing and repair. The main aspects for assessing the manufacturability that we adopt are i) the accessibility to different structural components, ii) the

required manufacturing processes and facilities, iii) and the price of the required components. The main components that comprise the flexible exoskeleton are carbon fibre rods and joints made of TPU 95A, as depicted in Figure 8.

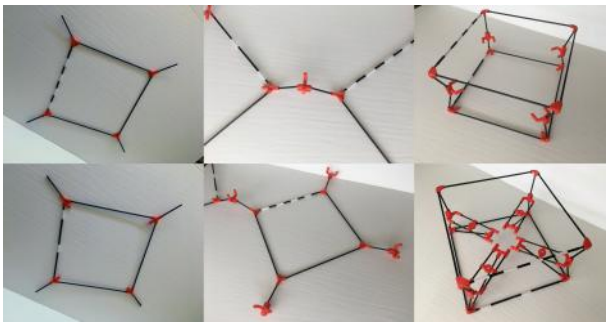

Fig. 8: The frame uses flexible 3D printed parts (shown above in red) that are printed flat and fold as you assemble the drone. The steps above illustrate how we assemble the outer frame mixing the flexible TPU parts with carbon fiber rods (left and center), finally folding and connecting top and bottom together (right). After the last step (right, bottom), it is necessary to add the rigid central 3D printed parts to have a full, ready-to-fly frame.

Carbon fibre rods are generally cheap, readily available, easy to cut and modify, and it is possible to find several examples of previous works using carbon fibre rods in drones [2], [13], [15]. We also use 3D printing, which is a versatile and affordable method that has become popular for designing drones [2], [10], [11], [12], [13], [14], [16], [15], [25], [26], [17], [18], [4]. A commercial-grade low-cost desktop 3D printer (e.g. Monoprice Mini v2) was used for printing the needed flexible joints out of TPU 95A filament, which proved to provide the desired flexibility and damping properties, in addition to the central body printed using more rigid plastics like ABS or PLA.

Since the beginning, our design efforts were focused on only using struts (diameter 3mm to match dollar store BBQ bamboo skewers, an affordable material useful for prototyping and testing as seen in Fig. 11) and 3D printed parts. However, the printed parts had to be easily printed using our small desktop 3D printer (printable volume of 120x120x120mm) based a Bowden extruder. Therefore, complex or big parts, or sometimes even the use of printed supports, had to be avoided.

To increase the success rate of 3D printed parts, specially flexible TPU ones, and to reduce laborious post-processing trimming, we envisioned a design where all parts but one (battery lid) are printed flat without the need of supports (Fig.10). That was possible by splitting the battery holder in two parts (with slots to easily post process using ordinary cyanoacrylate glue) and exploring the flexibility of the TPU 95A. Instead of complex parts using flexible filament, we took advantage of the material properties and designed the parts to bend (Fig. 8) or snap-fit (Fig. 9) as the drone was assembled. Another advantage of our design based on small parts is how easy it was to iterate and improve the design without the need to reprint (or rebuild) everything. All the 3D printed parts necessary to build CogniFly are depicted in Figure 10.

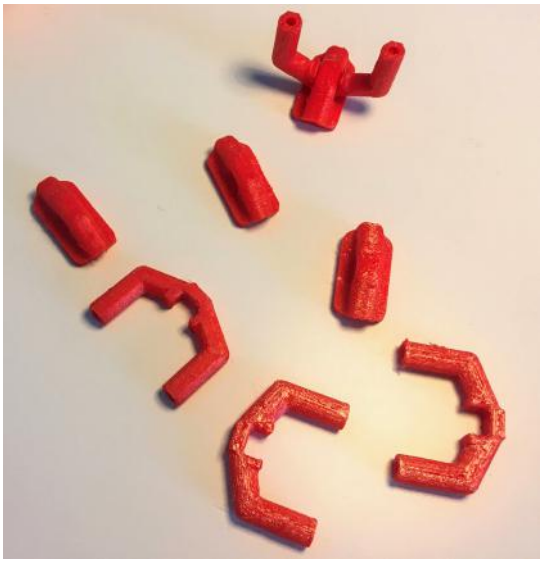

Fig. 9: Some 3D printed flexible parts (TPU 95A) are printed in two and snap-fit (squeezed) together afterwards creating one part with a hinge. Above can be seen the individual pieces before being squeezed together and the final part (top) that joins the arms holding the motors to our equivalent of an external cage.

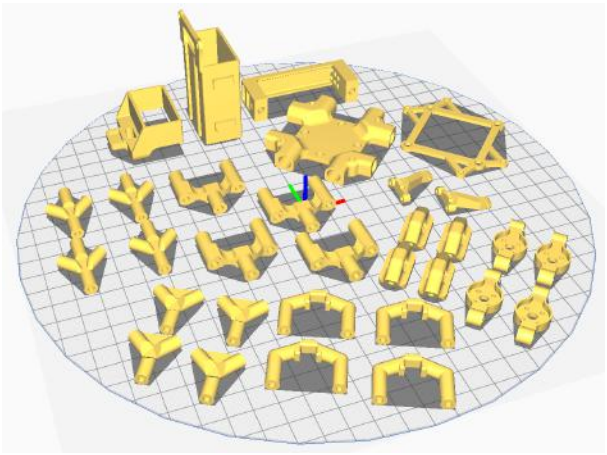

Fig. 10: All 3D printed parts (24 in TPU 95A, bottom and 7 in ABS/PLA, top) are shown on this 260mm diam. build plate. The biggest one is only 65x65x9mm. All parts, besides the small battery lid (top left), were designed to print flat and without the need for extra supports, drastically reducing the risk of failed printed parts.

B. Collision resilience

One of the main characteristics of the CogniFly is its ability to protect its payload, mainly through the absorbing impacts and limiting the transfer of impact energy to the payload when hitting obstacles directly. In the following, we present results of impact tests that show the CogniFly's ability to absorb impacts, as well as limit the maximum payload displacement during such impacts to demonstrate the protection aspect of CogniFly's design.

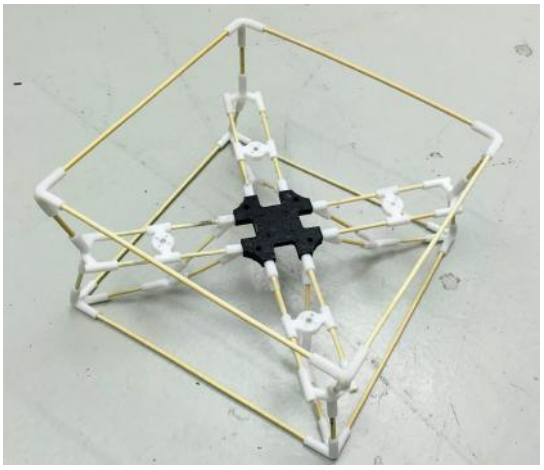

Fig. 11: 3D printed parts were designed to allow the use of carbon fiber rods as well as dollar store BBQ bamboo skewers (approx. diameter 3mm). Although more fragile than carbon fiber rods, bamboo is environmentally friendly, easy to cut and very affordable giving the user more freedom to explore new designs. The image above presents one early prototype using folding legs that was built entirely using bamboo instead of carbon fiber rods.

1) Impact testing: We reckon a vertical free fall to be a critical scenario as we consider payload contact with hard exterior objects, like the ground, has the highest potential of causing damage because the absolute acceleration values peak in such impact cases. Moreover, the battery is located at the bottom part of the drone, and should not subject to extreme loads which could result is a short-circuit of the battery's internal cells.

To demonstrate the flexible exoskeleton's ability to help dissipating impacts, we compare the CogniFly with a test item made with CogniFly's central body made of ABS (*rigid frame*). We carry out free fall tests for both setups from different altitudes and report boxplots of the peak acceleration onboard magnitude readings in Figure 12, which represent the severity of the impact [16].

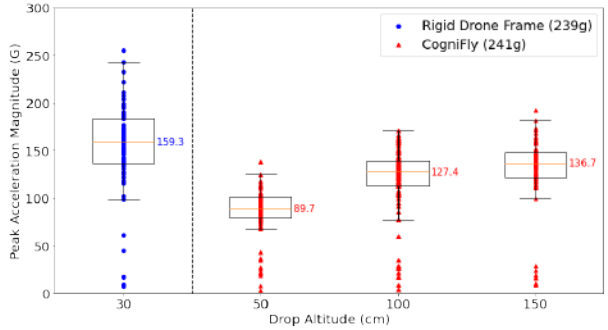

Fig. 12: Boxplot and scatter plot of all collected experimental crash landing peak acceleration data. Results show at least a five-fold $(150/30)$ improvement when comparing the median of CogniFly falls (right) from an altitude of $150\,\mathrm{cm}$ to a rigid structure falling from only $30\,\mathrm{cm}$ (left).

We carry out the free fall tests for the CogniFly at three different altitudes: $50\,\mathrm{cm}$, $100\,\mathrm{cm}$ and $150\,\mathrm{cm}$. To obtain usable data and avoid irreparable damage to the rigid frame, we limit its free fall to $30\,\mathrm{cm}$: pilot experiments using the rigid frame showed high risk of damage, and our accelerometer would saturate above $30\,\mathrm{cm}$. Figure 12 shows that the median of the absolute acceleration peak values for the rigid frame falling from $30\,\mathrm{cm}$ is higher than that of the CogniFly falling from $150\,\mathrm{cm}$. This proves the flexible exoskeleton (TPU joints and carbon fiber rods), is more capable of dissipating impacts than a rigid structure made of ABS plastic with almost equal weight.

As a final test, we tested CogniFly by dropping it from the maximum altitude our experimental setup allowed us (literally, our ceiling). Figure 13 shows a progression of payload displacement for a CogniFly free falling from 262cm, without suffering any damage (speed at impact of approximately $7\,\mathrm{m\,s^{-1}}$). Compared to some of the latest works on collision resilience UAVs with equivalent size and weight [14], [17], [16], [15], CogniFly reached the maximum collision speed without damages.

2) Payload maximum absolute acceleration: One of the main uses of the exoskeleton is to provide enough protection to the payload and more vulnerable components in worst case scenario impacts. The main criterion we adopt in this regard is the maximum absolute acceleration of the payload in case of a vertical free fall impact (i.e. crash landing), depicted in Figure 14.

In addition of being able to survive falls, the CogniFly has the ability to withstand in-flight side collisions and continue its mission (e.g. bouncing off walls) without the need for landing and resetting, unlike [16], [18], where the drone has to land before it is able to fly again because its motors are disconnected from the main body during collisions. The attached video demonstrates this ability through several collision tests.

C. Mass-spring-damper model

We model the CogniFly with its exoskeleton structure as a mass-spring-damper system, with the aim of predicting the distribution of energy stored and dissipated (Figure 17) as well as the displacement of the main payload after the beginning of the impact until the point the acceleration reaches its maximum value (Figure 16). A schematic of the model is depicted in Figure 14. The method we adopt for estimating the parameters from experimental data is described in the materials and methods section.

We assess the model by comparing the accelerometer readings onboard by the values of acceleration predicted by the model. Figure 15 compares the absolute acceleration of the proposed model with the measurement from the accelerometer. We compare accelerations as it is challenging to devise a reliable method for measuring the displacement of the center of gravity during impact, while we have easy access to precise accelerometer data. From a visual inspection of Figure 15, the predicted values follow the same trend as the experimental value's mean.

Since the main motivation behind the model is to predict the most critical failure mode (i.e. battery holder directly

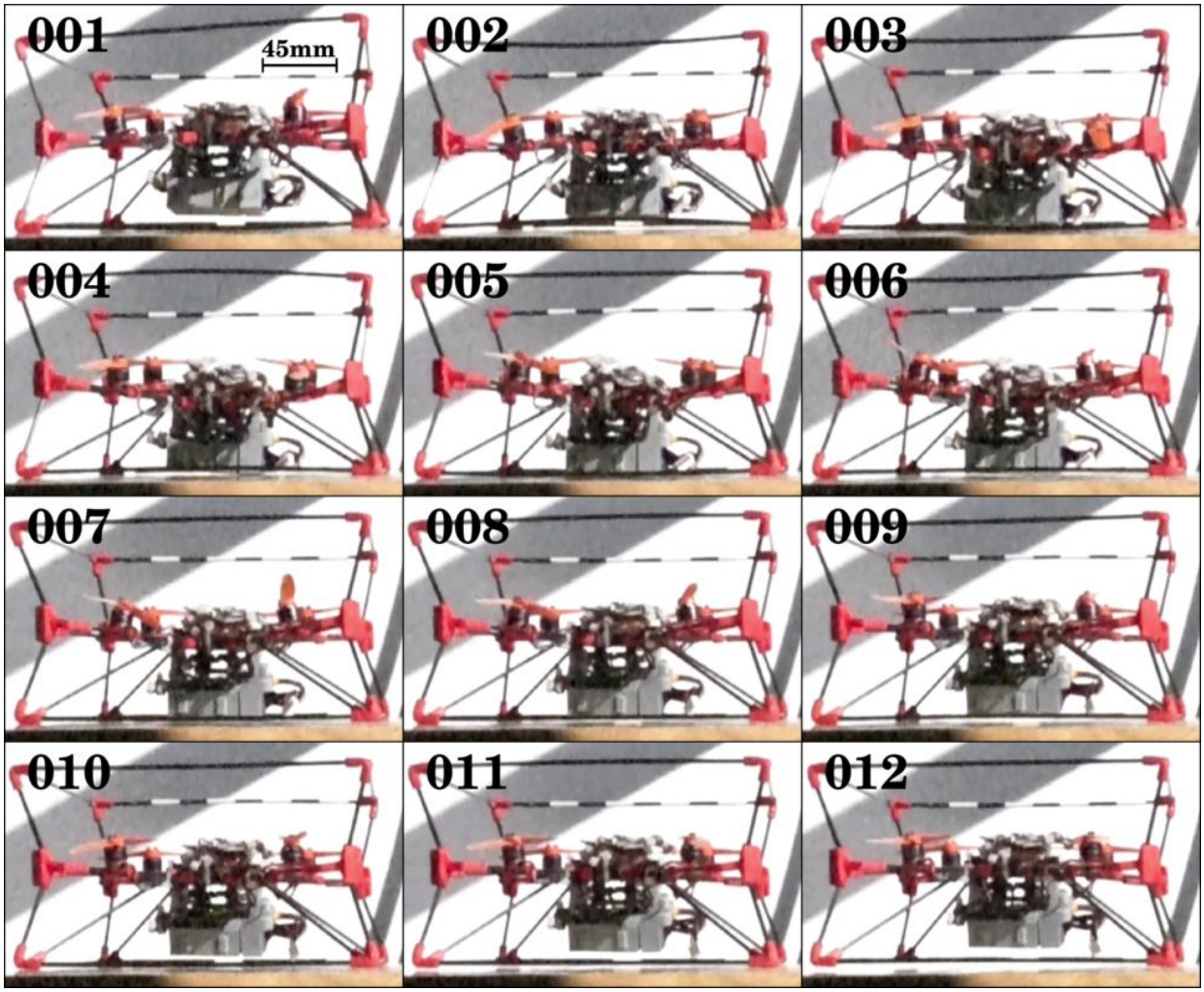

Fig. 13: Frames (960fps) of a fall from $262\,\mathrm{cm}$, mass of $241\,\mathrm{g}$ and speed at impact of approximately $7\,\mathrm{m\,s^{-1}}$. The structure bends in order to absorb the impact energy (frames 005 to 007), allowing the drone to survive without breaking its frame or any of the more fragile payload. Frames 008 to 012 show CogniFly bouncing back into the air, while still intact.

hitting the ground on free fall), Figure 16 shows the predicted payload's centre of gravity displacement after impact. The calculation of the predicted displacement and acceleration values is outlined in the Materials and Methods section. The allowable displacement for crash landing experiments presented in this paper (i.e. the maximum distance that can be travelled by the payload before hitting the ground) is 16mm, and Figure 16 predicts direct impacts on the battery holder for falls from altitudes equal or bigger to $150\,\mathrm{cm}$, which matches experimental results.

One of the uses of the proposed mass spring damper model is to explain and demonstrate the energy distribution in different parts of the drone for different altitudes, with the ability to predict such distribution for higher altitudes, which we demonstrate in Figure 17. We show that the fraction of the total kinetic energy at the point of impact is distributed in different components: the portion saved in the spring (in blue), the portion dissipated by the damper (in green), and the remaining portion that goes into collision (in red) for higher altitudes when the payload displacement is beyond the safe allowable value.

For altitudes below $150\,\mathrm{cm}$, Figure 17 shows that the total kinetic energy is divided between the damper and the spring, while for higher altitudes the amount of energy that goes into rigid collision increases with altitude. Such collision energy can give an indication of how strong the impact between payload and ground is, and this can help deciding how far the operational altitude of the drone can be pushed, had there been a need to go beyond a safe altitude.

IV. Discussion and Conclusions

In this paper, we introduce a new paradigm for collision resilient UAV design inspired by the flexible exoskeleton of arthropods, fusing the protective cage and the main frame in one semi-rigid structure with flexible joints that can withstand high-velocity impacts. Our UAV (Figure 1), weighs under $250\,\mathrm{g}$ and blends rigid and soft materials giving the final structure the ability to absorb and dissipate impact energy, while still being sufficiently stiff for agile flight. Thanks to its exoskeleton, it is possible to save precious payload capability when compared to a traditional protective cage design.

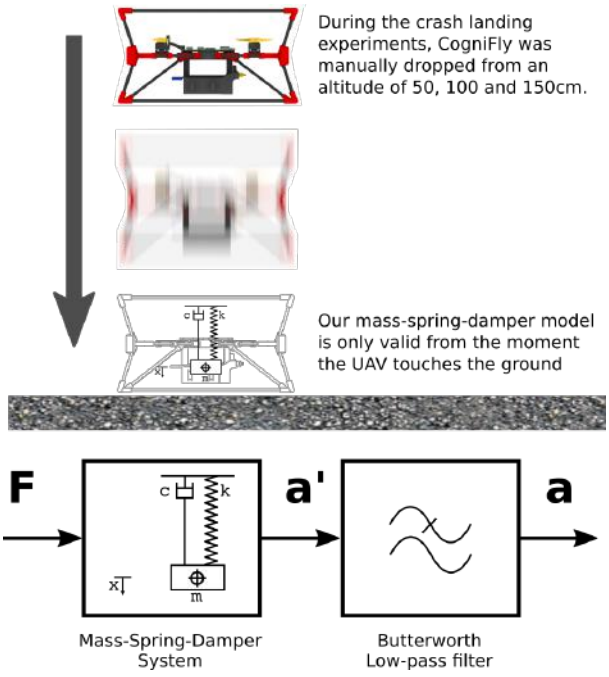

Fig. 14: Crash landing experiments were carried out by manually dropping CogniFly (as seen above) from 50, 100 and 150 cm. Acceleration data were collected using our customized data logger (Figure 4). Lumped Mass-Spring-Damper model (bottom) used to study the structure during crash landing tests considers the UAV hanging from the top (1 DOF). The model is valid while the external part of CogniFly's frame is touching the floor, but it doesn't account for a collision between rigid parts like the battery holder (when it initially touches the floor, $x_0 = 0mm$ and $v_0 = \sqrt{2 * g * h}$, where h is the drop altitude). A first order butterworth low pass filter (cutoff 500Hz) models the effect of the sampling latency.

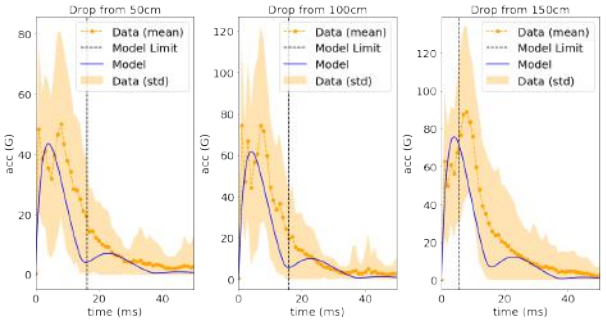

Fig. 15: Comparison of the raw measurements with our lumped model after passing through a first order Butterworth low-pass filter (cutoff 500Hz). Our model (Figure 14, $m = 0.241$, $c = 46$ and $k = 7040$) is valid while the frame is touching the floor ($t = 0$) or until its battery holder suffers a direct collision (black dashed line), that varies according to the drop altitude (Figure 16).

CogniFly survived multiple collisions at speeds up to $7\,\mathrm{m\,s^{-1}}$ while carrying enough computing power to run deep neural network models. Throughout a series of simple crash landing experiments (Figure 14), we show CogniFly withstands up to a five fold increase in the maximum collision energy when compared to a rigid system (3D printed on ABS) of similar weight. Moreover, we employ the experimental data to create a lumped mass-spring-damper model that allows us to extrapolate the results to untested cases while the calculated damping and stiffness can be used in to better understand the role of different materials or configurations.

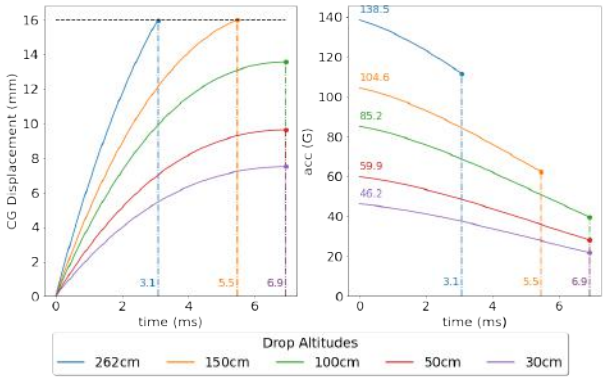

Fig. 16: CG displacements (left) and accelerations without low-pass (cutoff 500Hz) filter (right) calculated by our model (Figure 14, $m = 0.241$, $c = 46$ and $k = 7040$). Without the low-pass filter, accelerations wouldn't start at zero when the collision starts (t=0s).

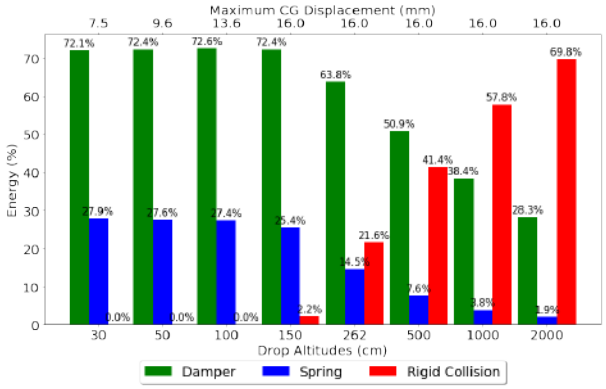

Fig. 17: Energy distribution according to the Mass-Spring-Damper model (Figure 14, $m = 0.241$, $c = 46$ and $k = 7040$). In this plot, we consider a collision when the CG displacement reaches 16mm. The results show a graceful degradation where the energy that will eventually cause a failure (collision) doesn't increases in steeply and even at 20m (2000cm) more than 25% of the initial potential energy will end up being dissipated (damper) and stored (spring) by the frame according to our model.

Our lumped mass-spring-damper model allows us to visualize the tradeoffs and where the energy is stored or dissipated as we extrapolate to impacts beyond our experimental data. These insights will be an useful tool to decide the next iterations of CogniFly's design (Figure17).

We designed CogniFly from the ground up for easy manufacturing and it can be built using a very small consumer-grade 3D printer, in addition to inexpensive off-the-shelf parts. Also, considering that batteries correspond to 33% of UAVs total

mass on average [21], our system was specifically designed to enable its battery to easily slide in and out for automatic swapping, which could theoretically allow continuous missions (Figure 2).

As an interesting side effect, we noticed an increased life span of the propellers used during our experiments. Throughout a period of almost one year crashing prototypes against walls, furniture and floors, we only used two sets of propellers (Gemfan 3025 3X2.5, Polycarbonate) with the second set seen in most images in this paper. One reasonable explanation for that is the flexibility of CogniFly's frame. Even the motors themselves are mounted on parts 3D printed using TPU 95A flexible filament. All that contributes to increase the time of impact, reducing forces, resulting in longer life spans for propellers.

Finally, as this is an open source project, all 3D files, software and data will be freely available on github under The CogniFly Project.

Future Work: The design of the drone itself was restricted by maximum weight (below $250\,\mathrm{g}$) and size (able to fit in a backpack without any disassembly, Figure 1). Future work possibilities would be to extend the model to take into account collisions from other directions, tune the design of the flexible parts to improve its collision resilience and analyze the impact of not being strictly stiff in the power consumption and dynamic reactions during flight. Ultimately, fatigue probably plays an important role in the structure's lifespan because some parts work as living hinges, therefore this would be another interesting topic to be further studied.

ACKNOWLEDGMENTS

We would like to thank the financial support received from IVADO (postdoctoral scholarship 2019/2020) and the productive discussions and help received from current and past students and interns from MISTLab.

REFERENCES

[1] Kaushik Jayaram, Jean-Michel Mongeau, Anand Mohapatra, Paul Birkmeyer, Ronald S Fearing, and Robert J Full. Transition by head-on collision: Mechanically mediated manoeuvres in cockroaches and small robots. *Journal of the Royal Society Interface*, 15(139):20170664, 2018.

[2] Adrien Briod, Przemyslaw Kornatowski, Jean-Christophe Zufferey, and Dario Floreano. A collision-resilient flying robot. *Journal of Field Robotics*, 31(4):496–509, 2014.

[3] Adrien Briod, Przemyslaw Kornatowski, Adam Klaptocz, Arnaud Garnier, Marco Pagnamenta, Jean-Christophe Zufferey, and Dario Floreano. Contact-based navigation for an autonomous flying robot. In *2013 IEEE/RSJ International Conference on Intelligent Robots and Systems*, pages 3987–3992. IEEE, 2013.

[4] Yash Mulgaonkar, Anurag Makineni, Luis Guerrero-Bonilla, and Vijay Kumar. Robust aerial robot swarms without collision avoidance. *IEEE Robotics and Automation Letters*, 3(1):596–603, 2017.

[5] Christos Papachristos, Shehryar Khattak, and Kostas Alexis. Haptic feedback-based reactive navigation for aerial robots subject to localization failure. In *2019 IEEE Aerospace Conference*, pages 1–7. IEEE, 2019.

[6] Thomas Lew, Tomoki Emmei, David D Fan, Tara Bartlett, Angel Santamaria-Navarro, Rohan Thakker, and Ali-akbar Agha-mohammadi. Contact inertial odometry: Collisions are your friend. *arXiv preprint arXiv:1909.00079*, 2019.

[7] Dhiraj Gandhi, Lerrel Pinto, and Abhinav Gupta. Learning to fly by crashing. In *2017 IEEE/RSJ International Conference on Intelligent Robots and Systems (IROS)*, pages 3948–3955. IEEE, 2017.

[8] Ali-akbar Agha-mohammadi, Andrea Tagliabue, Stephanie Schneider, Benjamin Morrell, Marco Pavone, Jason Hofgartner, Issa AD Nesnas, Rashied B Amini, Arash Kalantari, Alessandra Babuscia, et al. The shapeshifter: a morphing, multi-agent, multi-modal robotic platform for the exploration of titan (preprint version). *arXiv preprint arXiv:2003.08293*, 2020.

[9] Nikhil Khedekar, Frank Mascarich, Christos Papachristos, Tung Dang, and Kostas Alexis. Contact–based navigation path planning for aerial robots. In *2019 International Conference on Robotics and Automation (ICRA)*, pages 4161–4167. IEEE, 2019.

[10] Carl John O Salaan, Yoshito Okada, Shoma Mizutani, Takuma Ishii, Keishi Koura, Kazunori Ohno, and Satoshi Tadokoro. Close visual bridge inspection using a uav with a passive rotating spherical shell. *Journal of Field Robotics*, 35(6):850–867, 2018.

[11] Carl John Salaan, Kenjiro Tadakuma, Yoshito Okada, Yusuke Sakai, Kazunori Ohno, and Satoshi Tadokoro. Development and experimental validation of aerial vehicle with passive rotating shell on each rotor. *IEEE Robotics and Automation Letters*, 4(3):2568–2575, 2019.

[12] Arash Kalantari and Matthew Spenko. Design and experimental validation of hytaq, a hybrid terrestrial and aerial quadrotor. In *2013 IEEE International Conference on Robotics and Automation*, pages 4445–4450. IEEE, 2013.

[13] Adam Klaptocz, Adrien Briod, Ludovic Daler, Jean-Christophe Zufferey, and Dario Floreano. Euler spring collision protection for flying robots. In *2013 IEEE/RSJ International Conference on Intelligent Robots and Systems*, pages 1886–1892. IEEE, 2013.

[14] Pooya Sareh, Pisak Chermprayong, Marc Emmanuelli, Haris Nadeem, and Mirko Kovac. Rotorigami: A rotary origami protective system for robotic rotorcraft. *Science Robotics*, 3(22), 2018.

[15] Jiaming Zha, Xiangyu Wu, Joseph Kroeger, Natalia Perez, and Mark W Mueller. A collision-resilient aerial vehicle with icosahedron tensegrity structure. *arXiv preprint arXiv:2003.03417*, 2020.

[16] Stefano Mintchev, Sébastien de Rivaz, and Dario Floreano. Insect-inspired mechanical resilience for multicopters. *IEEE Robotics and automation letters*, 2(3):1248–1255, 2017.

[17] Jing Shu and Pakpong Chirarattananon. A quadrotor with an origami-inspired protective mechanism. *IEEE Robotics and Automation Letters*, 4(4):3820–3827, 2019.

[18] Stefano Mintchev, Jun Shintake, and Dario Floreano. Bioinspired dual-stiffness origami. *Science Robotics*, 3(20), 2018.

[19] Stefano Mintchev and Dario Floreano. A pocket sized foldable quadcopter for situational awareness and reconnaissance. In *2016 IEEE International Symposium on Safety, Security, and Rescue Robotics (SSRR)*, pages 396–401. Ieee, 2016.

[20] JaeHyung Jang, Kyunghwan Cho, and Gi-Hun Yang. Design and experimental study of dragonfly-inspired flexible blade to improve safety of drones. *IEEE Robotics and Automation Letters*, 4(4):4200–4207, 2019.

[21] Yash Mulgaonkar, Michael Whitzer, Brian Morgan, Christopher M Kroninger, Aaron M Harrington, and Vijay Kumar. Power and weight considerations in small, agile quadrotors. In *Micro-and Nanotechnology Sensors, Systems, and Applications VI*, volume 9083, page 90831Q. International Society for Optics and Photonics, 2014.

[22] Daniele Palossi, Antonio Loquercio, Francesco Conti, Eric Flamand, Davide Scaramuzza, and Luca Benini. A 64-mw dnn-based visual navigation engine for autonomous nano-drones. *IEEE Internet of Things Journal*, 6(5):8357–8371, 2019.

[23] Shuo Li, Erik van der Horst, Philipp Duernay, Christophe De Wagter, and Guido CHE de Croon. Visual model-predictive localization for computationally efficient autonomous racing of a 72-g drone. *Journal of Field Robotics*, 2020.

[24] Mary Ann Clark, Jung Ho Choi, and Matthew Douglas. *Biology 2e*. OpenStax College, Rice University, 2018.

[25] Stefano Mintchev, Davide Zappetti, Jérôme Willemin, and Dario Floreano. A soft robot for random exploration of terrestrial environments. In *2018 IEEE International Conference on Robotics and Automation (ICRA)*, pages 7492–7497. IEEE, 2018.

[26] Przemyslaw M Kornatowski, Stefano Mintchev, and Dario Floreano. An origami-inspired cargo drone. In *2017 IEEE/RSJ International Conference on Intelligent Robots and Systems (IROS)*, pages 6855–6862. IEEE, 2017.